applied sciences

MDPI

Article

Structure Design Improvement and Stiffness Reinforcement of a Machine Tool through Topology Optimization Based on Machining Characteristics

Shen-Yung Lin * and Chun-Ho Chang

Department of Mechanical and Computer-Aided Engineering, National Formosa University, 64, Wunhua Rd., Huwei Township 632, Yunlin, Taiwan; 40571128@gm.nfu.edu.tw
* Correspondence: sylin@nfu.edu.tw; Tel.: +886-919-051127

Abstract: Machining characteristics were applied to topology optimization for machine tool structure design improvement in this study, and the goals of lightweight and high rigidity of the structure were achieved. Firstly, an ultrasonic-assisted grinding experiment was carried out on zirconia to investigate the surface roughness, surface morphology, grinding vibration, and forces. Then, the topology optimization analysis was conducted for structure design improvement, in which the magnitude of the grinding vibration was utilized as the reference for selecting the topology subsystems and the grinding force was used as the boundary conditions of the static analysis in the topology optimization. Hence, columns, bases, and saddles were redesigned for structure stiffness improvement, and the variations in the effective stress, natural frequency, weight, and stiffness of the whole machine tool were compared accordingly. The results showed that the deduced topological shape (model) can make the natural frequency and stiffness of the whole machine tool tend to be stable and convergent with a weight retention rate more than 75% as the design constraint. The subsystem structures with larger effective stress distributions were designated for stiffness improvement in the design. At the same time, the topological shape (model) was also employed in the design for weight reduction, focusing on minimizing redundant materials within the structure. In contrast to the consistency of the modal shapes before and after topological analysis, the sequential number of the modal mode of the machine tool model after topological analysis was advanced by two modes relative to those of the original situation, which means the original machine tool may be out of its inherently resonant frequency range. Also, the natural frequencies corresponding to each mode had an increasing tendency, and the maximum increase was 110.28%. Furthermore, the stiffness of the machine tool also increased significantly, with a maximum of 355.97%, leading to minor changes of the machine tool's weight. These results confirm that the topology optimization based on machining characteristics proposed in this study for structure redesign improvement and stiffness enhancement is effective and feasible.

Keywords: machining characteristics; stiffness reinforcement; design improvement; topology optimization

check for updates

Citation: Lin, S.-Y.; Chang, C.-H. Structure Design Improvement and Stiffness Reinforcement of a Machine Tool through Topology Optimization Based on Machining Characteristics. *Appl. Sci.* **2024**, *14*, 61. https://doi.org/10.3390/app14010061

Academic Editors: Jun Yang, Lintao Wang and Jixiang Yang

Received: 22 November 2023
Revised: 9 December 2023
Accepted: 13 December 2023
Published: 20 December 2023

Copyright: © 2023 by the authors. Licensee MDPI, Basel, Switzerland. This article is an open access article distributed under the terms and conditions of the Creative Commons Attribution (CC BY) license (https://creativecommons.org/licenses/by/4.0/).

1. Introduction

In recent years, advancements in newly developed materials have further led to increased demands for their mechanical and physical properties. Hard and brittle materials such as superalloys, ceramics, quartz glass, and sapphires are thus produced. Due to the significant differences in their physical and mechanical properties as compared with metallic materials, traditional machining methods struggle to enhance machining efficiency and cost reduction simultaneously. As a result, the development of ultrasonic-assisted machining methods has emerged. This assisted machining approach can reduce the cutting force and friction resistance between the cutting tool and workpiece, thereby improving the machining quality. Furthermore, with the evolution of machining technologies, achieving high rigidity and a lightweight design have become crucial research topics in machine tool structural development. When designing a machine tool structure, it is essential to consider its rigidity and avoid the resonant frequencies that the machine tool may encounter during the machining process. As a result, the possibility of a machine tool's vibrating system causing environmental resonances may be minimized. Therefore, research into machining characteristics during cutting processes to investigate the interconnected relationship between machine tool structural rigidity and process dynamics is increasingly important. This interconnection could serve as a reference for machine tool structural design and manufacturing improvements. The ultimate goal of machining performance and efficiency promotions can be achieved accordingly.

Through the use of the finite element method for the design and analysis of milling tools, the principle of ultrasonic lateral vibration conversion for the transformation of vertical vibration power at the vibration node (the maximum pressure point) into lateral vibration is applied (2009). The necessary horizontal cutting force may thus be generated to optimize the removal efficiency of hard and brittle materials during abrasive grain milling. This also enables the design of more suitable cutting tools for milling processes. The milling tool shape, when expanded and scaled down during the machining stage, is fully incorporated after power conversion and can effectively enhance the cutting performance. Furthermore, under the same conditions of piezoelectric ceramics, changes in the existing vibration system can be made to achieve optimal performance. The results show that the conversion of vertical vibration power into lateral vibration effectively enhances the horizontal cutting force and the material removal is facilitated. To increase the swing of the vibration system, in addition to increasing the input pressure, a swing amplification shaft can be used to amplify the required swing. Therefore, modeling and designing the amplification shaft in finite element software for simulation analysis is necessary and the amplified value demonstrates a linear relationship with the theoretical values. The simulation of a vibration response in an ultrasonic vibration system with software could be coupled with appropriate elements such as common metal materials and quartz piezoelectric ceramics, and high accuracy could be achieved. The design time and manufacturing costs in practical manufacturing processes may thus be effectively reduced [1].

Wu et al. (2023) investigated the impact of ultrasonic vibration on the machining performance of titanium alloy experimentally in the hybrid-assisted grinding of ultrasonic vibration/plasma oxidation. In this experiment, a three-axis CNC machining center with an ultrasonic spindle at a frequency of 25 kHz attached to a conductive grinding wheel was utilized to perform ultrasonic vibration. It was connected to a plasma oxidation power supply and hybrid-assisted grinding of a titanium alloy was thus achieved. These results indicate that applying ultrasonic vibration and increasing the vibration amplitude can reduce the grinding forces. The reduction in grinding forces is more pronounced when plasma oxidation is employed. Since the ultrasonic cavitation effect can enhance the plasma intensity, the microhardness of the surface oxidized layer is further decreased. Simultaneously, there is a trend of reducing the surface roughness of the machined surface with an increase in vibration amplitude. The application of ultrasonic vibration assistance improves material removal rates, especially with a more significant effect under plasma oxidation conditions. The increase in material removal rates is attributed to a reduction in grinding forces during the vibration-assisted process, which subsequently diminishes deformations in the machining system. In the context of hybrid-assisted grinding of plasma/vibration, it was observed that the chip size became smaller and more granular. The efficient removal of chips from the grinding zone and the reduction of chip adhesion to the grinding wheel can be assisted by this improvement. With the increase in the vibration amplitude, there is a further promotion of chip adhesion reduction [2].

Gao et al. (2009) presented a novel ultrasonic grinding vibration device and established a theoretical model of surface roughness for ultrasonic vibration-assisted grinding. The impact of grinding parameters on the surface roughness was tested, and the micro-surface characteristics and critical ductile cutting depth with and without ultrasonic assistance were analyzed based on the experimental data and atomic force microscopy images. The experimental results indicate that in ultrasonic grinding, the effects of wheel velocity and grinding depth on surface roughness are similar to conventional grinding. A critical ductile cutting depth greater than that of conventional grinding and traditional ZrO_2 engineering ceramics was observed. These findings suggested that the use of nano-class scale ultrasonic assistance is feasible for the machining of nano-ZrO_2 ceramics [3].

Yang et al. (2019) employed ultrasonic vibration-assisted grinding as a non-traditional machining method for ceramic materials processing. A theoretical analysis of the trajectories during ultrasonic vibration-assisted machining was conducted. On this basis, the removal mechanism of zirconia in ultrasonic vibration-assisted grinding was investigated. Initially, nano-scratching tests with a single abrasive grain were conducted on ZrO_2 ceramic material. Experimental analysis revealed that the removal mode (plastic or brittle) of zirconia ceramic changed with increasing loads. Subsequently, based on the scratching tests and kinematic analysis of the ultrasonic vibration-assisted grinding (UVAG), a grinding force prediction model was established and the effectiveness of the model was validated through design experiments. It was observed that the grinding force decreased as the spindle speed and amplitude increased, while the grinding force increased as the feed rate and grinding depth increased. Furthermore, the grinding force significantly decreased in UVAG as compared to conventional grinding (CG). Experimental analysis also indicated an improvement in the surface quality of the workpiece and wear reduction of the grinding head in UVAG as compared to CG [4].

Huo et al. (2010) proposed a comprehensive approach for integrating dynamic modeling and numerical simulation to support the analysis and optimization of the overall machine dynamics and cutting performance during the early design phase. Based on this approach, the process of designing and modeling an innovative five-axis bench-top ultra-precision micro-milling machine was presented. This modeling and simulation encompass the machine structure, moving components, control system, and the dynamics of the cutting process. It was used to predict the overall machine tool dynamic performance for two typical machine configurations, open-frame and closed-frame. Through static analysis, modal analysis, and harmonic analysis of the machine tool structures for both open-frame and closed-frame bench-top machines, the static and dynamic loop stiffness of the machine structure was predicted and the effectiveness and feasibility of the proposed approach were validated. Preliminary cutting experiments also confirmed that this approach can ensure the right operation of the machine tool during its initial setup [5].

Zulaika et al. (2011) proposed an approach to ensure the minimization of the mass of the moving structural components of a large milling machine tool while maximizing material removal (targeted productivity). This design method involved an iterative design process that translated the productivity target requirements of the milling process into design optimization criteria, which guided the conceptualization of a large milling machine tool with the minimum possible mass of moving structural components while ensuring a stable cutting productive performance. A modeling approach was employed that used a stability model of the milling process in modal coordinates to model the interaction between the milling process and the machine tool structure. This model allowed for the identification of mechanical design parameters that limited the productivity and the threshold values required to meet the targeted productivity. These critical values were reached through an iterative procedure aimed at minimizing the mass of critical structural components in the machine tool. This methodology was applied to redesign an actual milling machine tool and machining tests were conducted. It resulted in a productivity increase of over 100% and a reduction in energy consumption by more than 20% due to the mass reduction of the moving structural components [6].

Li et al. (2012) developed a simple and practical method for the optimal design of a machine tool bed structure. First, establish a simplified fiber model composed of a shell and matrix elements to handle the numerical simulations of the complex mechanical structures and boundary conditions. Next, identify the load bearing path topology of the bed structure to represent the optimal layout of the internal stiffener ribs. Subsequently, utilize innovative optimization criteria that describe the best weight distribution for both the external support panels and internal stiffener ribs to produce a detailed sizing optimization design. The results demonstrated the effectiveness of the proposed method when using the example of a grinding machine tool bed as a design case [7].

Gupta et al. (2021) focused on the structural analysis of the hollow square column of three-sided and four-sided CNC machine tools. Various parameters were considered, such as a bionic design, total number of ribs and apertures, type of aperture, and tapering angles. The analysis concentrated on the stability, static structural analysis, and load effects of the CNC machine tool. The results of finite element analysis were compared with those in the literature. An optimization method using the derivative parameter approach was employed to determine the optimized ranking of the tested columns. With the assistance of software, successful static structural analysis was conducted. These research findings will contribute to the development of CNC machine tool structures. Based on the literature and finite element analysis results, the following conclusions can be drawn: based on the optimization criterion, which is the minimum value of the derivative parameter, a four-sided column with four horizontal plate ribs featuring rotated square-shaped apertures provides the best choice and is the optimal option among 14 competing cases. For the most rigid structure, i.e., the one with the minimum displacement, the best choice among the 14 competing cases was a four-sided column with an optimized wall thickness and four horizontal plate ribs without any apertures. To design a lightweight structure, it was recommended to use a three-sided column with a tapered back and a wall thickness of 25 mm, with a refined taper angle of 12.99, no back side, and no ribs. This structure was the lightest among the 14 competing cases and had less material volume [8].

Kroll et al. (2011) investigated the impact of lightweight design measures on the energy efficiency of machine tools. After a comprehensive elaboration and categorization of the primary lightweight design measures for machine tool energy efficiency, different strategies for achieving a maximum reduction of the mass of machine tool structural components through lightweight design were considered. Subsequently, the direct and indirect effects of lightweight design measures were discussed in more detail, which accounted for their quantitative impact on energy efficiency. Through sensitivity analysis, the potential for a direct reduction of electrical energy consumption in feed drives and the potential for an indirect reduction in base load through improved performance to decrease energy losses in machine tool auxiliary systems were explored. Finally, based on static stiffness, the actual components of an existing medium-sized machine tool were redesigned and the optimized components were integrated into the finite element model of the entire machine tool. Their dynamic behavior and their impact on electrical energy consumption were studied through mechatronic simulations. The results showed that a structural lightweight design could achieve up to a 30% reduction in the mass of the structural components, while a material lightweight design could lead to a reduction in the mass of the structural components by up to 50% of the structural component itself. Considering the steel deposits required for functional purposes and the several devices that must be moved with the structural components such as servo drives, auxiliary systems, energy chains, etc., the overall potential for mass reduction in the moving part of the feed drive is typically less than 30% [9].

Ji et al. (2020) proposed a structural design optimization method for energy-efficient CNC machine tool moving components. Firstly, an energy consumption characteristic model for the machine tool moving components was explicitly established, and a structural optimization design model for the moving components was developed with energy consumption and static and dynamic performance as objectives. Secondly, a comprehensive approach was employed, incorporating a uniform design method, sensitivity analysis, response surface methodology, and principal component analysis to comprehensively construct a structural optimization model for the moving components. This enabled a better understanding of the interaction mechanisms of structural parameters on energy consumption and structural performance. Finally, a hybrid algorithm combining particle swarm optimization (PSO) and simulated annealing (SA) was proposed to solve the optimization model, and the convergence speed and global search capability were significantly improved and ensured, respectively. Through the analysis and simulation of the optimization results, it was concluded that the proposed optimization method for moving components can achieve the same energy-saving effect as the lightest structure while enhancing the static and dynamic performance of the moving components [10].

Huang et al. (2011) conducted a parametric design for a gantry milling machine tool column by using the APDL language in ANSYS. Subsequently, a finite element model of the column was created for static analysis. Based on this analysis, a topology optimization method for the column structure was proposed, which led to the development of an optimal design approach for weight minimization. A subsequent finite element analysis was performed to analyze the reconfigured column structure. Through structural topology optimization, the stress distribution in various parts of the column became more homogeneous and reasonable. Without altering the stress and rigidity, the weight of the column was reduced by approximately 10% [11].

Gao et al. (2011) focused on a high-speed machining center's worktable study. To meet the overall performance requirements of the high-speed machining center, a 3D model of the worktable was created in SolidWorks (version 2017). Subsequently, static analysis and modal analysis were conducted in ANSYS Workbench. The worktable was optimized by using the topology optimization module in ANSYS Workbench. The results indicated an improvement in the worktable's structure. The optimized worktable maintained its original static rigidity performance while enhancing its dynamic performance. Additionally, the original structure weight was reduced to achieve a better worktable design [12].

Ding et al. (2010) proposed an optimal design approach for a machine tool bed structure, which consisted of three stages: first, a reasonable and simplified model called the "fiber model" was applied to optimize the layout of stiffener plates within the bed structure. Second, detailed sizing optimization was performed on the stiffener plates and support blocks under the bed. Third, a topology design optimization for the distribution of the manufacturing hole in bed structure was executed. A typical cylindrical grinding machine tool bed was chosen as an example to validate the proposed method. The results demonstrated the effectiveness of this approach, and it led to an improvement in the structural eco-efficiency [13].

Zhao et al. (2008) used a structural bionic approach based on the configuration principles of biological skeletons and plant stems to redesign the stiffener ribs of a machine tool column to improve its static and dynamic performance. After verifying the lightening effects through finite element simulations, scaled-down models of both the conventional column and the bionic column were manufactured and tested. The results showed that both the maximum static displacement and mass could be reduced, and a better dynamic performance with an increase in the first two natural frequencies was exhibited for the bionic column. Structural bionic design proved to be effective in enhancing the static and dynamic structural performance of high-speed machine tools [14].

Kovalov et al. (2016) proposed a method for arranging the frame of a heavy-duty lathe to distribute forces along the coordinate axes loads that act on the machine tool during operation. A three-dimensional mathematical model of the large bearing system for the heavy-duty lathe was developed, which accounts for typical and boundary loads. On-site tests were conducted to analyze the frame's movement along the coordinate axes under high loads. Physical modeling and study of the support structure for the heavy-duty lathe were carried out using simulation software. A method for studying the composite bed accuracy through mathematical modeling was developed. By using the preliminary calculation results as boundary conditions of contact deformation for designing individual load-bearing structures, a support structure technique for heavy machinery was designed. The design geometry of the cross section with the lowest possible weight while meeting specified performance and precision machining standards was achieved and allowed. The results showed the design of a high-precision heavy-duty lathe frame with a load capacity of 100 tons, capable of machining up to 12.5 m in length and 2.5 m in diameter, with a maximum cutting force of 200 kN. Recommendations for designing CNC high-precision heavy-duty machine tool bearing systems were provided [15].

Sharma et al. (2023) conducted a study to examine structural optimization of machine tools using finite element analysis. The stability of the structure under the influence of cutting forces is crucial for achieving machining precision. To initiate the investigation, a machine tool structure was created, and cutting forces were estimated for different wood and aluminum samples using an energy method. Initially, static and dynamic analyses were performed on the initial structure, and maximum displacement values and modal frequencies were recorded. Subsequently, structural optimization was carried out by using stiffener plates with a fixed mass constraint rate of the initial volume. The optimized structure was reanalyzed and reductions of the maximum static and dynamic displacements were achieved. Furthermore, the modal frequencies of the optimized structure increased as compared to the original structure, which increased the gap with excitation frequencies and thereby avoided resonance occurrence. That study aimed to analyze the placement of the stiffener plates using finite element analysis techniques to reduce the overall weight and enhance the stability of the machine tool structure, providing insights into the optimization of machine tool structures [16].

Kiyono et al. (2023) introduced a new approach to address stress-based topology optimization problems by utilizing a binary structural topology optimization method. Design updates were performed using binary values (0 or 1), and a boundary identification scheme was employed to smooth the structural contours, avoiding artificial stress concentrations caused by the rugged nature of the topology optimization process. Due to boundary identification, re-meshing was required at each iteration. To minimize discontinuities in the moving domain during the iterative process, a two-domain technique, as presented by Picelli et al.'s TOBS (topology optimization of binary structures)—GT (geometric trimming) methodology was followed. Two distinct domains were defined: the first was an extension domain (referred to as the topology domain) that remains fixed and is meshed only at the beginning of the optimization process. The second was the trimmed domain with identified structure boundaries (referred to as the analysis domain), which needs to be meshed at each iteration for displacement and stress calculations using finite element methods. Within this mesh, a variable called pseudo-density is defined for each element, even though there are no void elements in the analysis domain. Spatial filtering techniques were applied to prevent numerical instability and extrapolate the void region. Numerical examples were provided to demonstrate the efficiency of this approach. The results indicated that the proposed trimming and remeshing domain method successfully addresses optimization problems where considering strength criteria can become troublesome, mitigating the rugged boundary transition between void and phase materials [17].

Amaral et al. (2022) employed first-order reliability method-based displacement and stress limit state functions for reliability analysis to quantify uncertainties in material properties, applied load and geometric parameters, and determined new optimized topologies through the proportional topology optimization (PTO) method. The innovation lies in incorporating the framework of reliability-based design optimization into topology optimization within a dual-loop scheme. Reliability analysis serves as the inner loop within the topology optimization outer loop. The PTO method was applied to analyze beams based on bidirectional evolutionary structural optimization. Moreover, a sensitivity analysis was conducted to assist in revealing the relative importance of uncertain variables in the final reliability within the design decisions of the topology optimized structures. Failure probabilities and corresponding reliability indices of the optimized geometries were obtained in numerical examples of a simply supported beam and a double-clamped beam. The results demonstrated the importance of considering reliability constraints in the final topology to ensure a safe and cost-effective design [18].

Many researchers have proposed various methods for structural design and numerical refinement analysis, which are highly beneficial and worth referencing for structural design improvement. However, this study adopted a practical approach based on machining characteristics, systematically conducting topology optimization analysis and structural stiffness enhancement design step-by-step. In this study, topology optimization based on machining characteristics was applied for structural design improvement of a machine tool. The machining characteristics, such as grinding vibrations, grinding forces, and surface roughness obtained from the ultrasonic-assisted grinding experiments of zirconia were utilized as the boundary conditions in static analysis. Both equivalent stress distributions obtained from static analysis and the geometric shape (model) after topological analysis were utilized as the key references for further structural design improvement of the column, base, and saddle subsystems. The differences of the effective stress, natural frequency, corresponding modal shape, weight and stiffness of a machine tool between the original structure and after design improvement may thus be compared completely.

The method proposed in this study may closely align with the dual requirements of structural stiffness enhancement and the pursuit of a lightweight design for machine tools. The proposed procedures also may serve as a practical reference to direct the industry manufacturer in enhancing the design of existing machine tools or contribute to the development of the next generation of machine tools.

2. Theoretical Foundation

This section introduces the principles of grinding, ultrasonic-assisted machining, and topology optimization, and the relevant procedures.

2.1. Grinding

Grinding is a machining process that utilizes abrasive grits with significantly higher hardness than the workpiece material to grind the workpiece. Grinding can achieve better machining accuracy, surface roughness, and a high level of machining allowance for precision machining requirements. In the grinding processes of hard and brittle materials, abrasive grits come into contact with the workpiece and then rubbing, ploughing, and cutting actions are generated sequentially to remove the materials, as shown in Figure 1. Additionally, diamond tools are commonly used for grinding of hard and brittle materials due to their high hardness and wear resistance. Grinding processes generally can be divided into the following three stages:

1. Rubbing stage: due to the internal stress within the workpiece material not reaching the fracture threshold, elastic and plastic deformation is caused by the rubbing of diamond abrasive grits and the workpiece material is not removed at this stage.
2. Ploughing stage: workpiece material is extruded outwardly toward both sides and the front end of the diamond abrasive grit when the cutting force induces plastic deformation in the workpiece. As a result, cracks and a small amount of material are removed.
3. Cutting stage: cracks in the workpiece continue to propagate, which causes lateral cracking on the workpiece material surface to be generated. These lateral cracks are subsequently detached and chips are thus formed that are removed at this stage.

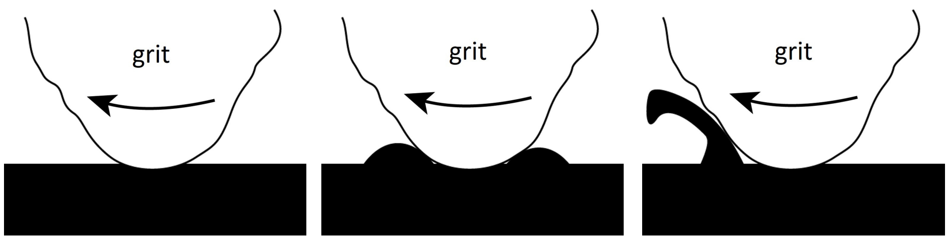

(**a**) Rubbing (**b**) Ploughing (**c**) Cutting

Figure 1. Grinding processes of abrasive grit.

During the grinding processes, electroplated diamond coating burs can exhibit different grinding patterns due to influential factors such as grain size, structure (texture), bond strength, and the type of abrasive material used. Clogging and blunting are more likely to occur when conditions involve a finer grain size, higher structure, and harder bond strength. Diamond abrasive grits in the grinding processes can generally be categorized into the following types:

1. Detachment: due to excessive grinding forces, the bonding agent is damaged and the detachment of abrasive grits thus occurs.
2. Partial grit damage: some abrasive cutting edges are damaged due to grinding forces. The grinding performance deteriorates as the size of this damage exceeds the amount of wear.
3. Significant damage and wear: a substantial loss of abrasive grits causes the abrasive region to become cutting edges, and the cutting-edge area is thus reduced.
4. Flattening: wear and abrasion occurs due to the high-temperature friction between the grinding edge and the workpiece and a flattened appearance is gradually formed.
5. Newly emerged: the wear of the bonding agent leads to the exposure of the abrasive grit during the grinding process and a new cutting edge emerges.

2.2. Ultrasonic-Assisted Machining

Ultrasonic-assisted machining, as a new technology distinct from traditional machining, can be regarded as an advanced and complex cutting process primarily applied to hard and brittle materials. Its characteristics not only include lower cutting temperatures and reduced cutting forces but also high-frequency vibrations that facilitate self-cleaning of the cutting tool, preventing chip build-up and enhancing machining precision.

In machining processes, simply adding cutting fluid may have limited actual improvement in machining performance. However, introducing ultrasonic-assisted cutting can significantly enhance both machining performance and cutting-tool life. This is because, in vibrational machining, a vacuum region is formed between the cutting tool and the workpiece and a pumping suction effect is thus formed in this region, as shown in Figure 2. Hence, the cutting fluid is likely to reach the primary cutting zone by this pumping suction effect.

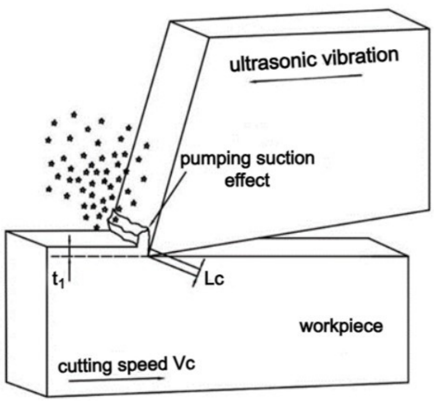

Figure 2. Schematic diagram for ultrasonic-assisted cutting.

2.3. Topology Optimization

This study employed a topology optimization method using the density function approach, wherein material density is treated as a design variable in structural design. A relationship between the material density and Young's modulus is established for each finite element. The density function approach, based on material interpolation, involves penalty factors and can be further categorized as solid isotropic material with penalization (SIMP) and rational approximation of material properties (RAMP). Therefore, this method is also referred to as the penalty function-based density function approach. The ANSYS

Workbench R18.1 software can automatically determine which interpolation method to use, with SIMP as shown in Equation (1) and RAMP as shown in Equation (2).

$$E = \rho^P E_0 \tag{1}$$

$$E = E_0 \frac{\rho}{1 + P(1-\rho)} \tag{2}$$

where ρ is the specific density value of the element ranges from 0 to 1, and 0 indicates the absence of the element while 1 indicates its presence. E_0 is the real Young's modulus for the materials. E is used to determine the Young's modulus during the topology optimization process. P as a penalty factor, it typically ranges from 2 to 4, with a default value of 3 in the software.

Based on the above information, it can be observed that when the penalty coefficient is greater than one, elements with lower specific density undergo an exponential operation, causing their E-values to decrease, facilitating their removal from the system. Ultimately, this allows for the optimization of the topological shape (model) based on different density distributions.

SIMP and RAMP methods primarily involve the steps of setting design variables and defining objective functions in the context of topology optimization. Specifically: 1. design variable setting: in the SIMP method, design variables are typically associated with the material density of each element. The material density of each element serves as a design variable that can be adjusted during the optimization process. Similar to the SIMP method, in the RAMP method, design variables are also related to the material density of each element. The material density of each element is used to describe the topological distribution. 2. Objective function definition: in the SIMP method, the objective function usually involves minimizing the deformation or volume of the structure. This is achieved by adjusting the material density of each element. The definition of the objective function often includes a relationship between the density and material properties, introducing a penalization factor to control the material distribution. The objective function is related to the relationship between the density and material properties. However, as compared to the SIMP method, the RAMP method introduces rational approximation to more accurately describe the material properties. The objective function involves minimizing the deformation or volume of the structure and utilizes rational approximation of the material properties. Therefore, both methods play a crucial role in the design variable and objective function definition stages of topology optimization. The choice between these methods often depends on the specific engineering requirements and the need for accurate representation of the material properties.

Structural optimization is a process of iteratively solving finite element models by continuously updating design variables and modifying the finite element model to meet the design requirements based on the constraint conditions. Topology optimization, during the analysis process, continuously modifies the material density within the optimization domain, effectively removing elements from the analysis model to achieve the optimization objectives.

Optimization analysis must be conducted with well-defined objective function and constraints in place, requiring a standardized procedure for the smooth execution of the optimization analysis. There are mainly four parameters involved:

1. Optimization region: seek the optimal material distribution within a given design area by applying the following three parameters.
2. Objective function: the objective function is the optimization target. It is defined as the quantity to be minimized or maximized based on the parameters in the design response. The objective function can also be expressed using multiple design responses, and in the case of multiple objective functions, weighting factors can be used to define the influence of each objective function on the system.
3. Response constraints: constraints imposed on the design response to fulfill the analysis or practical requirements, such as volume or weight reduction by a certain percentage.

4. Geometric constraints: also known as manufacturing constraints, they refer to the limitations imposed directly on design variables. These constraints are primarily imposed to ensure that the analyzed structure aligns with real-world requirements. They encompass factors such as member size, pull-out direction, extrusion limits, and symmetry limits.

Applying the SIMP and RAMP methods in ANSYS Workbench involves specific configurations for design variables and objective functions. Below are the general steps for utilizing the SIMP and RAMP methods in Workbench: 1. Design variable setting: open ANSYS Workbench and import or create the structural model in SIMP, access the topology optimization module, and select the structural domain for optimization. Designate the material density of each element as a design variable and specify the upper and lower limits for density, which can be adjusted during optimization. The RAMP method is similar to SIMP: treat the material density of each element as a design variable, and set upper and lower limits for density. 2. Objective function definition: choose the performance index for optimization in SIMP, such as minimizing structural deformation or volume. The objective function typically involves density distribution and material properties. By using a penalization factor to adjust the relationship between density and material, apply Young's modulus for optimization. Unlike SIMP, when using the RAMP method, introduce a rational approximation of the material properties and configure the objective function to minimize structural deformation or volume while considering the influence of rational approximation. 3. Constraint setting: set constraints based on specific requirements, such as maximum stress, degree of freedom limitations, etc. The constraints setting may ensure that the optimization results comply with the design requirements. 4. Select the optimization algorithm: in Workbench, choose an appropriate optimization algorithm, such as sequential quadratic programming (SQP), genetic algorithm (GA), etc.

2.4. Relevant Procedures

A flowchart demonstrating the overall relevant procedures performed in this study is depicted in Figure 3.

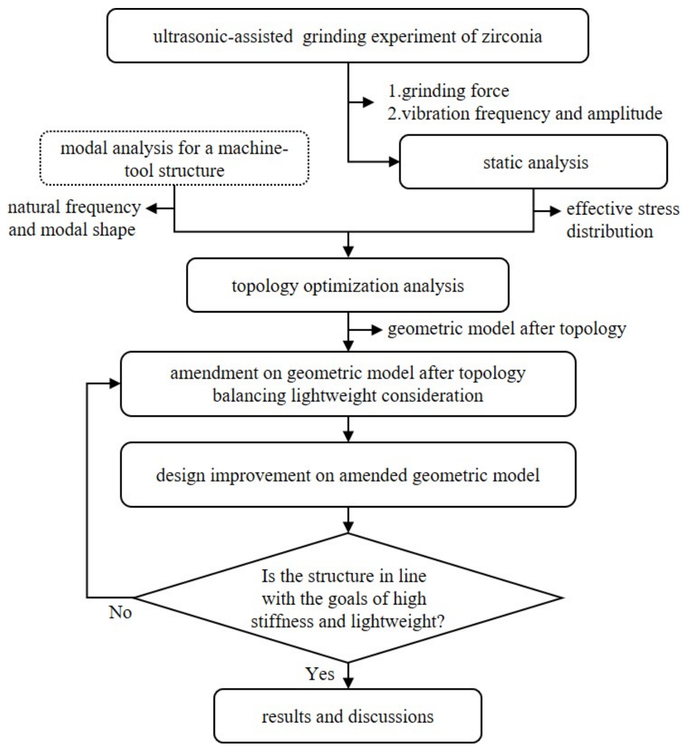

Figure 3. Flowchart for the overall relevant procedures performed in this study.

3. Ultrasonic-Assisted Grinding Experiment

Due to the focus of this study on the variations of machining characteristics, an ultrasonic-assisted machining technique was introduced in the grinding experiment and the cutting vibrations and forces were detected and acquired accordingly. These machining characteristics serve as the foundational factors for structural optimization analysis, which is an important assisted reference for subsequent structural design improvement aimed at fulfilling the stiffness reinforcement and lightweight requirements in the machine tool structure.

3.1. Experimental Setup and Process Planning

The schematic and images of the experimental setup for ultrasonic-assisted grinding of a difficult-to-cut material such as zirconia are shown in Figures 4 and 5, respectively. A dynamometer (Kistler 9257B, Kistler Group, Winterthur, Switzerland) is mounted between the worktable and the vice-fixture to monitor the grinding forces. The signal detected from the dynamometer is transmitted to a charge amplifier (Kistler 5070A) and a signal acquisition card (NI-9215, National Instruments Co., Austin, TX, USA), and finally, it is recorded on a laptop for the measurement of grinding forces. Grinding vibrations are detected using a three-axis accelerometer (B&K 4506B, Brüel & Kjær, Nærum, Denmark) to capture the relative vibrations between the workpiece and grinding tool. Its signal is then transmitted to a spectrum analyzer (B&K 3560C) and recorded on a laptop for the measurement of grinding vibrations. The grinding process parameters for the experiment are planned as shown in Table 1. Additionally, the hammer impact on each subsystem of casting iron and the whole machine tool for experimental modal analysis (EMA) was carried out in this study. As a result, the modal parameters of the structure can be obtained from the analysis results, and the corresponding modal shape of the structure can be established accordingly.

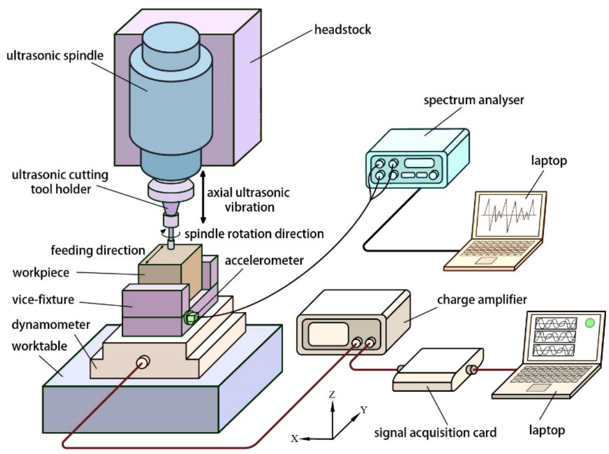

Figure 4. Schematic diagram of the experimental setup for ultrasonic grinding.

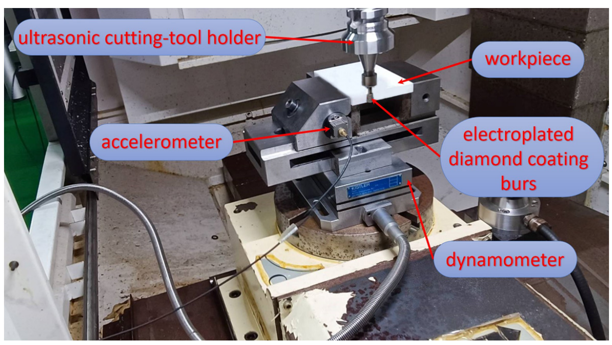

Figure 5. Image of the experimental setup for ultrasonic grinding.

Table 1. Process parameter planning for zirconia grinding.

Workpiece	zirconia
Grinding tool	electroplated diamond coating burs
Diameter of diamond coating burs (mm)	ψ8
Spindle speed(rpm)	18,000
Axial depth of cut(mm)	0.05
Feed rete (mm/min)	200 (roughing), 100 (finishing)
Ultrasonic vibration frequency(kHz)	25

3.2. Grinding Experimental Results

The machining characteristics obtained from the grinding experiment, such as grinding vibrations and grinding forces, were utilized both for topological objects (subsystems) selecting in subsequent topology optimization analysis and the boundary condition setting for the static analysis, respectively.

The vibration signals along different axial directions detected from ultrasonic-assisted roughing grinding of zirconia are shown in Figure 6. It can be observed that the vibration along the x-axis is not pronounced, while the vibration along the y-axis exhibits a slight vibration between 4 k to 6 kHz. The vibration along the z-axis is more prominent, particularly concentrated around 5 kHz. Therefore, 5 kHz is recognized as a reference frequency for further investigation of the vibration modal shapes of the machine tool, as depicted in Figure 7. From the numerical modal analysis, the six modal shapes around 5 kHz for a machine tool system model are shown in Figure 7. It reveals that the larger vibration subsystems in this machine tool are the column, base, and saddle. Hence, these three subsystems were designated as the objects for subsequent topology optimization analysis to enhance the overall machine tool rigidity, pursuing the lightweight goal simultaneously.

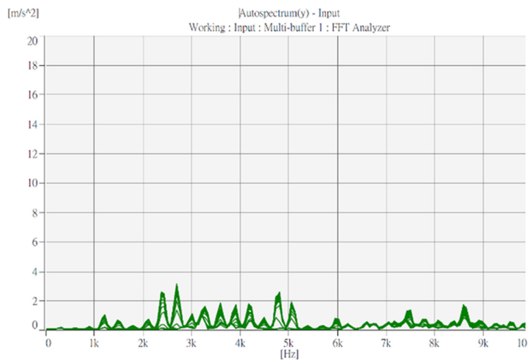

(**a**) x-axis

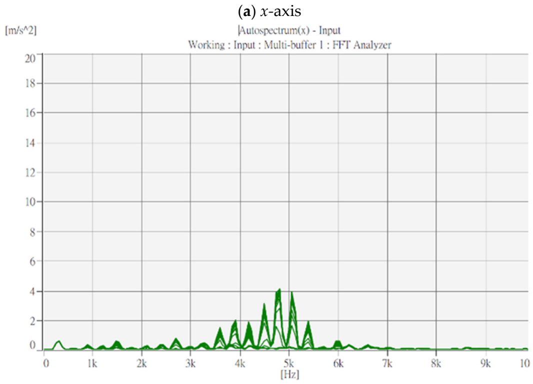

(**b**) y-axis

Figure 6. *Cont.*

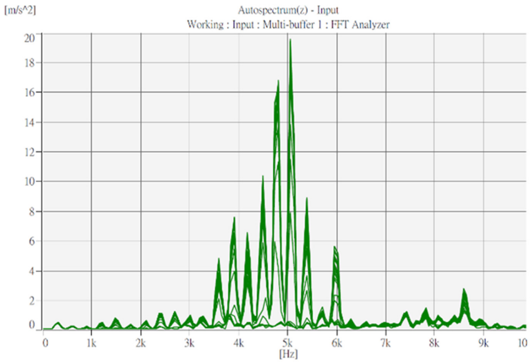

(**c**) *z*-axis

Figure 6. Vibration signals along different axial directions detected from the ultrasonic-assisted grinding process under the roughing grinding condition.

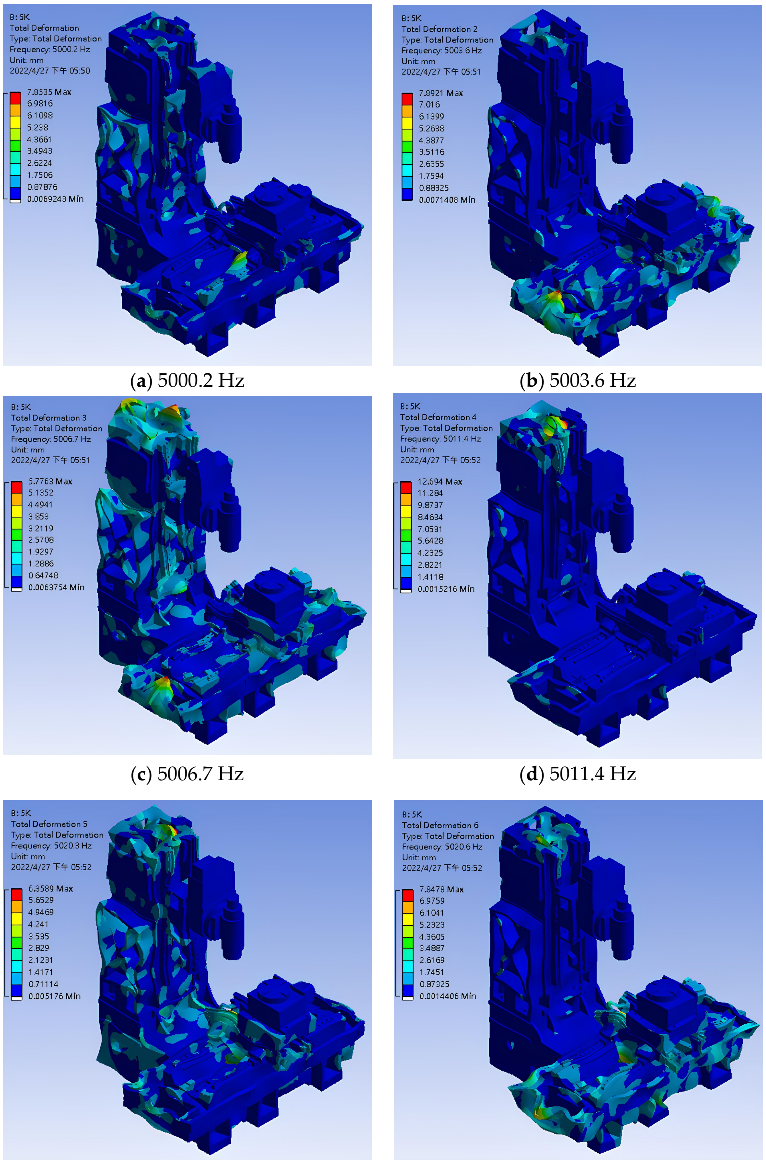

(**a**) 5000.2 Hz (**b**) 5003.6 Hz

(**c**) 5006.7 Hz (**d**) 5011.4 Hz

(**e**) 5020.3 Hz (**f**) 5020.6 Hz

Figure 7. Six modal shapes around 5 kHz for the machine tool system model.

After having conducted the ultrasonic-assisted roughing grinding experiments on a zirconia workpiece, the average measured surface roughness was 0.649 μm. Since the topological optimization analysis is strongly correlated with the results of the equivalent stress distributions, the grinding forces measured in roughing grinding experiments shown in Table 2 were utilized as the boundary conditions for the static analysis. The topological optimization was conducted separately for the x, y, and z axes, with a focus on the z-axis, where the grinding force is most prominent. Hence, the experimental results along the z-axis direction will be the main concerns for promoting the structural design improvement.

Table 2. Roughing grinding forces along different axial directions for zirconia.

Zirconia	x-Axis	y-Axis	z-Axis
Grinding force(N)	4.492	4.652	61.438

4. Topology Optimization Design

In topology optimization design, the optimization module in ANSYS Workbench is employed to conduct static analysis on the machine tool model. Based on the larger equivalent stress distributions, subsystems for which the structural design improvement should be performed are identified first. Subsequently, topology optimization analysis is performed, accounting for constraints and design variables to obtain a preliminary lightweight structure model (topological shape). Finally, both structure stiffness enhancement and weight reduction of the machine tool model are performed simultaneously based on some industrially practical design rules. Thus, the natural frequencies and the related stiffness of the whole machine tool system may be effectively promoted.

4.1. Topological Analysis

Based on the machining characteristics of the grinding vibrations and forces measured from the experiments, a topology optimization analysis was subsequently performed on the geometrical model of the machine tool system.

As mentioned above, the measured grinding forces along three axes were applied as the boundary conditions for the static analysis. In order to reflect the rationality and realistic situations of the grinding processes in static analysis, it is assumed that the spindle system will experience a reaction force due to the grinding forces. Therefore, reverse forces were applied on both the worktable and spindle systems along each axial direction when the boundary conditions were set in the static analysis. Figure 8 is a schematic representation of this setup.

The equivalent stress distributions were individually determined for the column, base, and saddle subsystems along each axial direction for which the grinding forces were applied separately. The results of the effective stress obtained from the numerical simulations along the different axial directions for the column subsystem are shown in Figure 9, while those obtained for the base and saddle subsystems are shown in mboxcreffig:applsci-2760055-f010,fig:applsci-2760055-f011, respectively. From Figures 9–11, it can be observed that stress concentrations always occurred around the structure turning corners or at the interfaces between the component connections, which may be regarded as the weak areas of the structure.

Figures 12–14 show the individual geometric shapes (models) after topological analysis at a 75% weight retention rate for the column, base, and saddle subsystems along each axial direction, respectively. That is, by using the equivalent stress distributions obtained from the static analysis, the above analyses were subsequently performed, applying the 75% weight retention rate constraints and design variables.

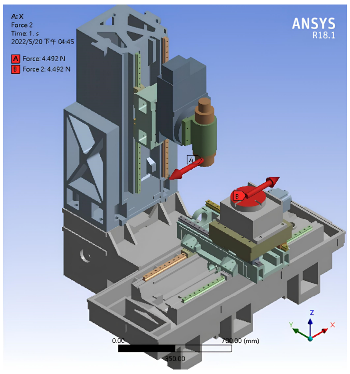

(**a**) *x*-axis

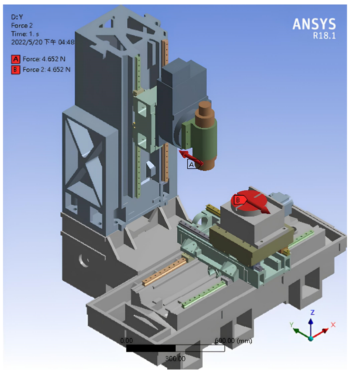

(**b**) *y*-axis

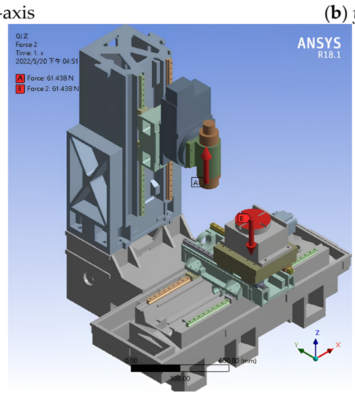

(**c**) *z*-axis

Figure 8. The grinding forces along different axial directions are applied to the worktable and spindle system oppositely.

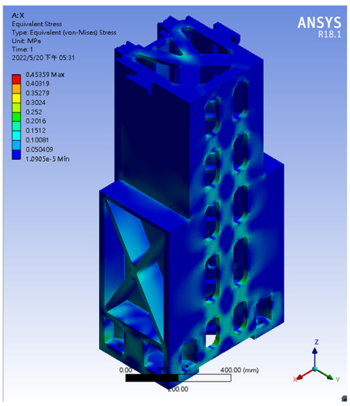

(**a**) *x*-axis

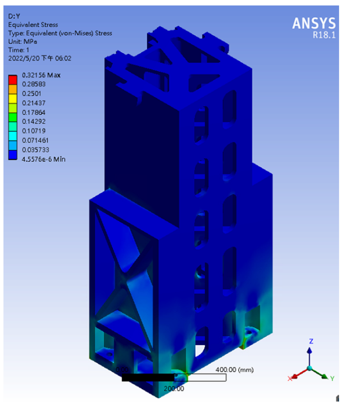

(**b**) *y*-axis

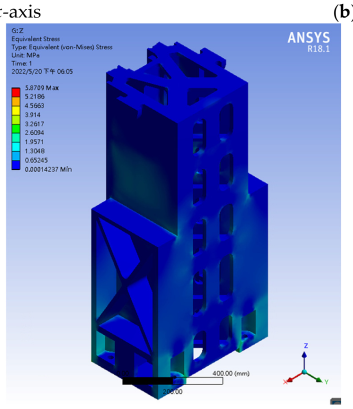

(**c**) *z*-axis

Figure 9. Equivalent stress distributions along different axial directions for the column subsystem.

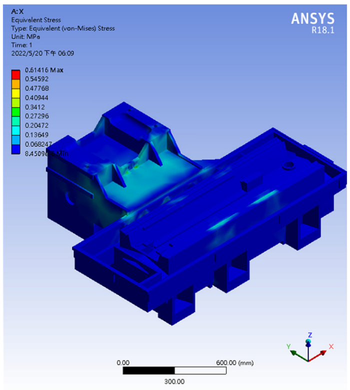
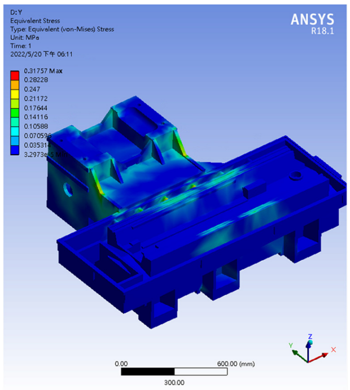

(**a**) *x*-axis (**b**) *y*-axis

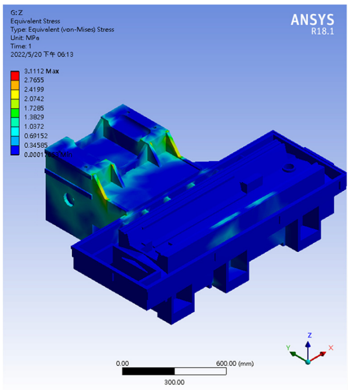

(**c**) *z*-axis

Figure 10. Equivalent stress distributions along the different axial directions for the base subsystem.

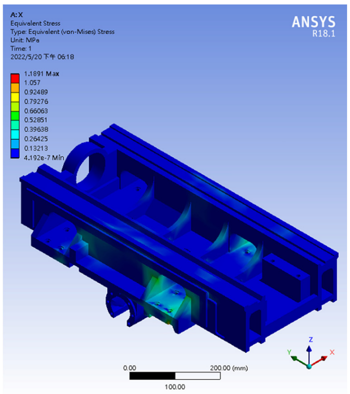
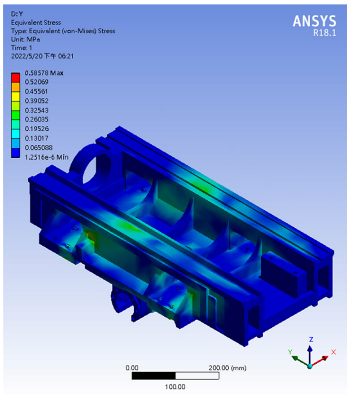

(**a**) *x*-axis (**b**) *y*-axis

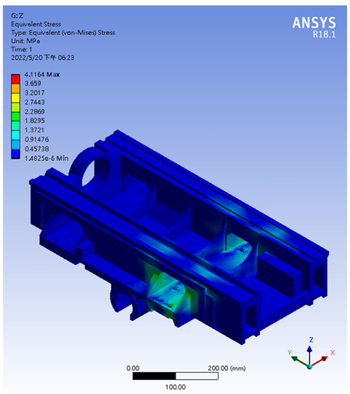

(**c**) *z*-axis

Figure 11. Equivalent stress distributions along the different axial directions for the saddle subsystem.

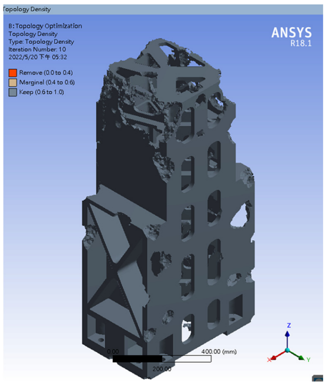

(**a**) x-axis

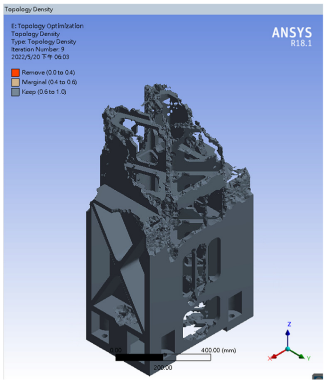

(**b**) y-axis

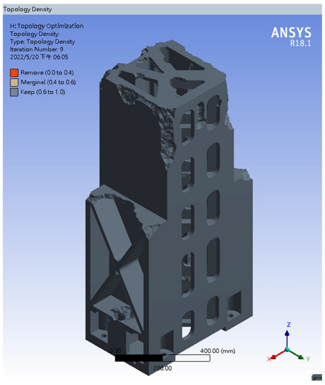

(**c**) z-axis

Figure 12. Geometric shape (model) after topological analysis along different axial directions for the column subsystem.

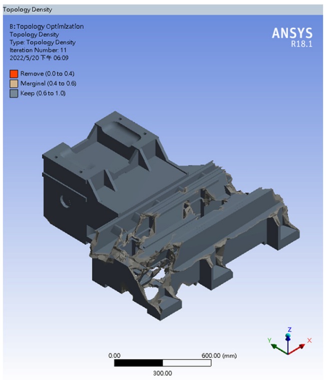

(**a**) x axis

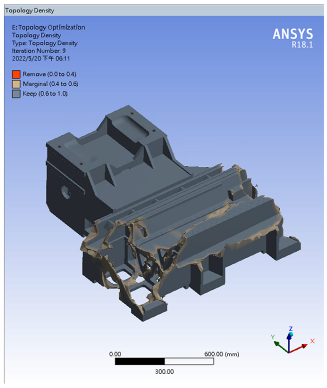

(**b**) y axis

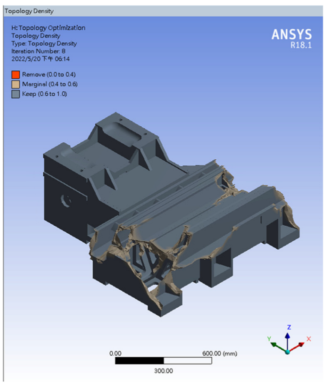

(**c**) z axis

Figure 13. Geometric shape (model) after topological analysis along different axial directions for the base subsystem.

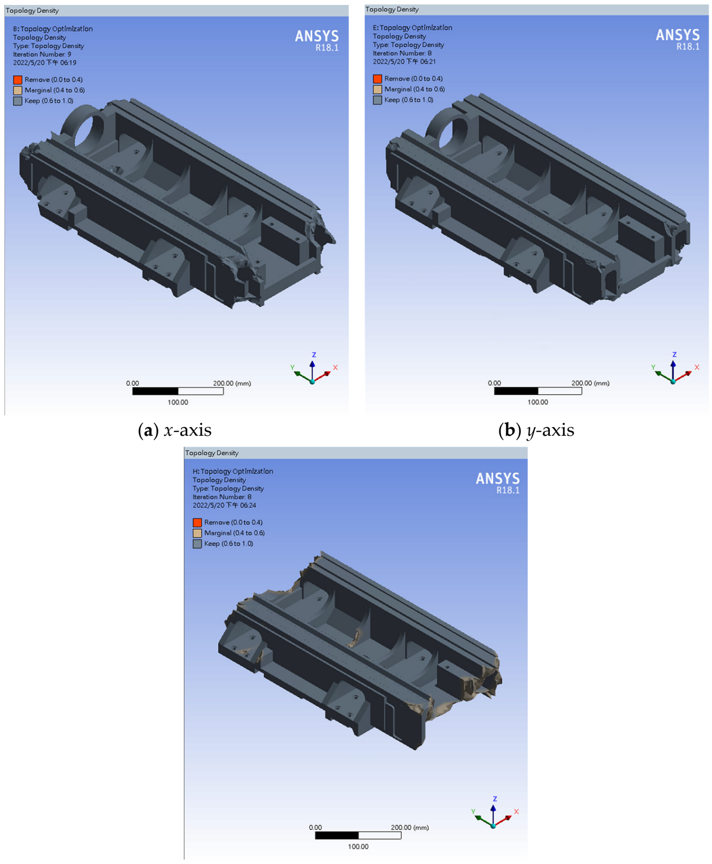

(**a**) x-axis (**b**) y-axis

(**c**) z-axis

Figure 14. Geometric shape (model) after topological analysis along different axial directions for the saddle subsystem.

4.2. Structural Design Improvement

After topological analysis, the amendments and reinforcements of the geometric shape (model) of these three structural subsystems were further performed by focusing on the areas with the equivalent stress concentrations. Additionally, for the areas in these structural subsystems that have been topologized, a rational lightweight design was also conducted based on the above amendment and reinforcement rules. Thus, the goals of lightweight and high rigidity may be achieved.

The following key points for structural design improvement can be derived from the above perspectives:

1. Based on the magnitude of the grinding forces along different axial directions as well as the effective stress distributions, and the geometric shape (model) after topological analysis, the priority order for structural design improvement is determined.
2. The effective stress distributions are utilized as a reference for structural design reinforcement.
3. The geometric shape (model) after topological analysis is also utilized as a reference for structural lightweight design.
4. The design considerations for the inner ribbed structure within the machine tool are primarily for withstanding loads with a secondary focus on lightweight construction, while those for the outer panel structure are primarily for lightweight construction with a secondary focus on supporting loads.

Taking the column subsystem as an example, Figures 15 and 16 illustrate the geometrical models before and after the design improvements for the column subsystem, respectively. The capsule-pattern is altered by the rhombus pattern on the outer panel behind the column subsystem at the structural redesign reinforcement stage, which will more effectively withstand the cutting force impacts along the x-axis direction during machining. Moreover, a single-arm structure on both sides of the middle section of the column subsystem has been added, which may be better able to resist the impacts of cutting forces from the y-axis and z-axis directions during machining. This enhanced modification is based on the features of the effective stress distributions. Additionally, the protruding structures on both sides have been altered from the rectangular to trapezoidal shapes. Both lightweight and inner ribbed structure strengthening may be conducted and achieved simultaneously in this study. Similar structural redesign improvement procedures have also been applied to the base and saddle subsystem models, as depicted in Figures 17 and 18, which follow the same design rule considerations and methods as the column subsystem.

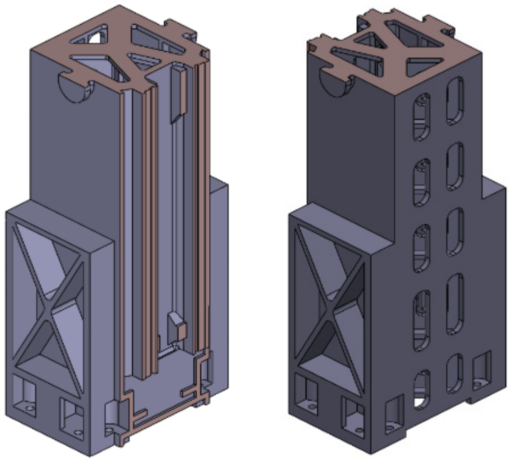

Figure 15. Geometrical model before design improvement for the column subsystem. Left to right: front and back sides.

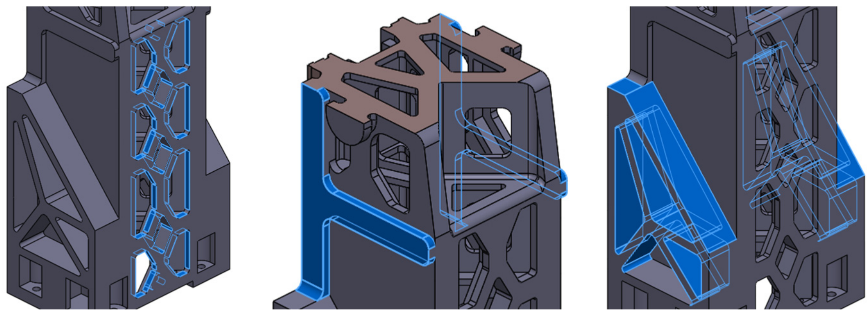

Figure 16. Geometrical models after design improvements for the column subsystem. Left to right: from the capsule-like to the rhombus-pattern on the back side outer panel, single-arm structure, from the rectangular to the trapezoidal shapes.

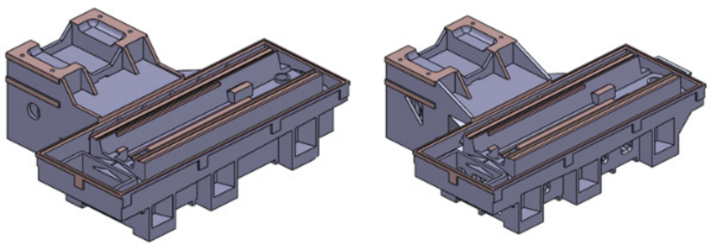

Figure 17. Geometrical models before and after design improvements for the base subsystem. Left to right: before design improvements, after design improvements.

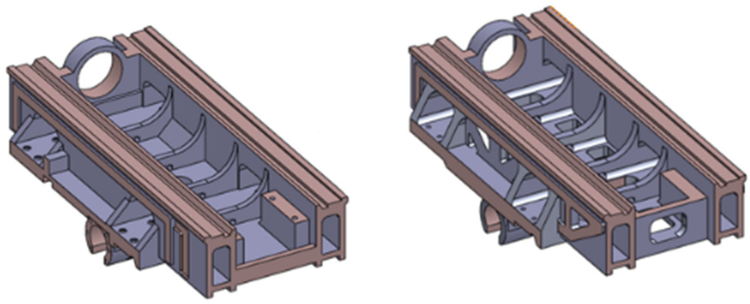

Figure 18. Geometrical models before and after design improvements for the saddle subsystem. Left to right: before design improvements, after design improvements.

4.3. Variations in Effective Stress, Natural Frequency, and Rigidity

Both the effective stress distributions resulting from the actions of the grinding forces along different axial directions in the static analysis and the geometric shape (model) after topological analysis are integrated to determine the selection priority for structural design improvement. Thus, the structure areas of a machine tool with larger effective stress distributions may be identified and the relevant subsystem emerge for stiffness reinforcement and improvement design. The geometric shape (model) after topological analysis can be used concurrently as a reference for a lightweight structure design. On this basis, comparison of the locations of maximum effective stress between the original structure and after design improvement for a machine tool system subjected to different direction loadings is shown in Table 3. The maximum effective stresses all occurred at the same locations of the subsystem before and after the design improvement. Moreover, the maximum effective stresses were all reduced after design improvement, and the maximum variation was about 25% along the z-axis direction.

Table 3. Comparison of the locations of the maximum effective stress between the original structure and after design improvement for a machine tool system.

Loading Direction	Original Structure		After Design Improvement		Variation (%)
	$\bar{\sigma}_{max}$ (MPa)	Location	$\bar{\sigma}_{max}$ (MPa)	Location	
x	2.083	column	2.059	column	−1.15
y	2.795	saddle	2.221	saddle	−20.53
z	28.358	column	21.331	column	−24.77

The relationship between the natural frequency, mass, and stiffness is represented by $k = \omega^2 m$, where k represents the stiffness (N/mm), ω is the natural frequency (Hz), and m is the mass (kg). The unit of ω can also be expressed in terms of angular velocity (rad/s = 1/s) and m can also be derived from the formula $m = F/a$ and its unit is Ns^2/m.

The comparisons of the natural frequencies before and after the structural design improvement of a whole machine tool system are shown in Table 4. The corresponding modal shapes are depicted in Figure 19. Since the comparisons of the natural frequencies are based on the condition of having quite similar modal shapes, increasing the modal number order not only enhances the overall natural frequencies but also allows the entire machine tool system model to be out of its inherently resonant frequency range. This will avoid the occurrence of structure resonance. Moreover, there was a slight increase in natural frequencies for the six modes (modes from the 3th to 8th after the design improvement contrast with those from the 1st to 6th before the design enhancement), with the largest increase being 110.28%.

Table 4. Comparison of natural frequencies between the original structure and after design improvement for a machine tool system.

Original Structure		After Design Improvement Column + Base + Saddle		Variation (%dd)
Mode	Natural Frequency (Hz)	Mode	Natural Frequency (Hz)	
1	70.75	3	137.76	94.72
2	88.63	4	186.37	110.28
3	131.16	5	212.87	62.30
4	174.98	6	246.92	41.11
5	204.74	7	320.52	56.55
6	250.12	8	339.35	35.67

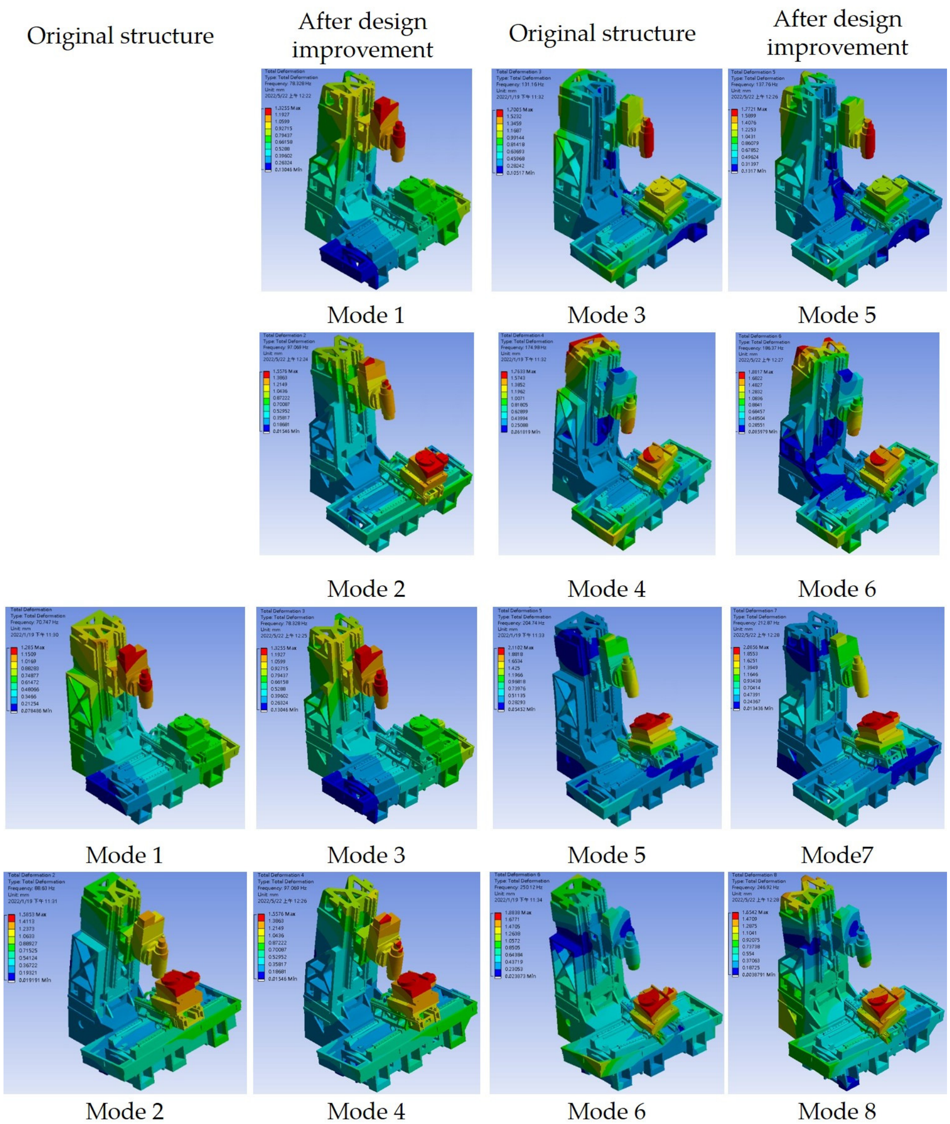

Figure 19. Comparison of modal shapes between the original structure and after design improvement for a machine tool system.

The weight comparison before and after the structural design improvement of a machine tool system is shown in Table 5, while the stiffness comparison corresponding to each mode is shown in Table 6. It can be observed that the maximum variation in stiffness may be achieved up to 355.97% in the case of topology optimization of the column, base, and saddle subsystems when concurrently integrated together. This confirms that the topology optimization based on machining characteristics proposed in this study for structural design improvement and stiffness enhancement is feasible and effective.

Table 5. Comparison of weight between the original structure and after design improvement for a machine tool system.

Original Structure (kg)	After Design Improvement (kg) Column + Base + Saddle	Variation (%)
2417	2492.4	3.12

Table 6. Comparison of stiffnesses between the original structure and after design improvement for a machine tool system.

Original Structure		After Design Improvement Column + Base + Saddle		Variation (%)
Mode	Stiffness (N/mm)	Mode	Stiffness (N/mm)	
1	1.21×10^7	3	4.73×10^7	291.00
2	1.90×10^7	4	8.66×10^7	355.97
3	4.16×10^7	5	1.13×10^8	171.62
4	7.40×10^7	6	1.52×10^8	105.34
5	1.01×10^8	7	2.56×10^8	152.72
6	1.51×10^8	8	2.87×10^8	89.82

The variations, φ, of the effective stress, natural frequencies, weight, and stiffnesses of a machine tool are defined as:

$$\varphi = \frac{after\ design\ improvement - original\ structure}{original\ structure} \tag{3}$$

The variations of the effective stress, natural frequencies, weight, and stiffnesses of a machine tool obtained from the finite element analyses are calculated by Equation (3) and shown in Tables 3–6, respectively. It is defined as the difference between the numerical simulation result after design improvement and that before design improvement, and then divided by the simulation result before design improvement (the original structure).

5. Conclusions

Topology optimization based on machining characteristics was applied for structural design improvement and relevant stiffness reinforcement of a machine tool. The machining characteristics such as grinding vibrations and forces obtained from the ultrasonic-assisted grinding experiments of zirconia were utilized as the structure vibration investigations and boundary condition setting in static analysis, respectively. Both equivalent stress distributions obtained from the static analysis and the geometric shape (model) after topological analysis were utilized as important references for further structural design improvement of the column, base, and saddle subsystems. The differences in the effective stress, natural frequency, corresponding modal shape, weight, and stiffness of a machine tool between the original structure and after the design improvement may thus be compared completely. From the above analyses, the following conclusions can thus be drawn:

1. Machining characteristics were successfully applied to topology optimization in this study. Through experiments, the grinding vibration was detected, and the distinct frequencies obtained were employed for modal shape investigations in numerical modal analysis. The subsystems of a machine tool system with larger displacement may thus be identified, such as the column, base, and saddle for further topology optimization.

Meanwhile, the grinding forces measured during the experiments can be utilized for boundary condition setting in the static analysis for topological optimization.

2. Through topology optimization analysis, a comparison of a machine tool structural model before and after design improvements revealed that, under the consistency conditions of modal shapes, the sequential mode number was advanced by two modes after design improvement. This means the original machine tool after design improvement may be out of its inherently resonant frequency range. Furthermore, after design improvement, the natural frequency in each mode experienced an increasing phenomenon, with a maximum improvement of 110.28%. Despite only a minor increase in the machine tool weight, the stiffness of the entire system exhibited a significant increase, with a maximum improvement of 355.97%. This confirms the applicability and effectiveness of the proposed method and the accompanying procedures for topology optimization analysis in this study.

Author Contributions: Conceptualization, supervision, writing, S.-Y.L.; methodology, analysis, C.-H.C. All authors have read and agreed to the published version of the manuscript.

Funding: The authors acknowledge the National Science and Technology Council for their support in this research under the grant of MOST 109-2622-E-150-011.

Institutional Review Board Statement: Not applicable.

Informed Consent Statement: Not applicable.

Data Availability Statement: Correspondence and requests for materials should be addressed to Shen-Yung Lin. The data are not publicly available due to patent in review.

Conflicts of Interest: The authors declare no conflict of interest.

References

1. Kuo, K.L. Ultrasonic vibrating system design and tool analysis. *Trans. Nonferr. Met. Soc. China* **2009**, *19*, s225–s231. [CrossRef]
2. Wu, H.; Duan, W.; Sun, L.; Zeng, J.; Li, S.; Wang, Q.; Wu, Y.; Chen, Y. Effect of ultrasonic vibration on the machining performance and mechanism of hybrid ultrasonic vibration/plasma oxidation assisted grinding. *J. Manuf. Process.* **2023**, *94*, 466–478. [CrossRef]
3. Gao, G.F.; Zhao, B.; Xiang, D.H.; Kong, Q.H. Research on the surface characteristics in ultrasonic grinding nano-zirconia ceramics. *J. Mater. Process. Technol.* **2009**, *209*, 32–37. [CrossRef]
4. Yang, Z.; Zhu, L.; Lin, B.; Zhang, G.; Ni, C.; Sui, T. The grinding force modeling and experimental study of ZrO_2 ceramic materials in ultrasonic vibration assisted grinding. *Ceram. Int.* **2019**, *45*, 8873–8889. [CrossRef]
5. Huo, D.; Cheng, K.; Wardle, F. A holistic integrated dynamic design and modelling approach applied to the development of ultraprecision micro-milling machines. *Int. J. Mach. Tools Manuf.* **2010**, *50*, 335–343. [CrossRef]
6. Zulaika, J.J.; Campa, F.J.; Lopez de Lacalle, L.N. An integrated process–machine approach for designing productive and lightweight milling machines. *Int. J. Mach. Tools Manuf.* **2011**, *51*, 591–604. [CrossRef]
7. Li, B.; Hong, J.; Wang, Z.; Wu, W.; Chen, Y. Optimal design of machine tool bed by load bearing topology identification with weight distribution criterion. *Procedia CIRP* **2012**, *3*, 626–631. [CrossRef]
8. Gupta, M.; Goswami, C.; Khandelwal, N. Design and structural analysis of 3-sided and 4-sided columns of a CNC machine using finite element analysis. *Mater. Today Proc.* **2021**, *47*, 5895–5900. [CrossRef]
9. Kroll, L.; Blau, P.; Wabner, M.; Frieß, U.; Eulitz, J.; Klärner, M. Lightweight components for energy-efficient machine tools. *CIRP J. Manuf. Sci. Technol.* **2011**, *4*, 148–160. [CrossRef]
10. Ji, Q.; Li, C.; Zhu, D.; Jin, Y.; Lv, Y.; He, J. Structural design optimization of moving component in CNC machine tool for energy saving. *J. Clean. Prod.* **2020**, *246*, 118976. [CrossRef]
11. Huang, W.; Ou, C.S.; Lu, H.M.; Xie, Z.L. Finite element analysis and topology optimization for the gantry milling machine column structure. *Appl. Mech. Mater.* **2011**, *80–81*, 1016–1020. [CrossRef]
12. Gao, D.Q.; Zhang, F.; Mao, Z.Y.; Lin, H.; Yi, J.M. Finite element analysis and structure optimization of machine tool worktable. *Appl. Mech. Mater.* **2011**, *80–81*, 985–989. [CrossRef]
13. Ding, X.; Chen, Y.; Liu, W. Optimal design approach for eco-efficient machine tool bed. *Int. J. Mech. Mater. Des.* **2010**, *6*, 351–358. [CrossRef]
14. Zhao, L.; Chen, W.Y.; Ma, J.F.; Yang, Y.B. Structural bionic design and experimental verification of a machine tool column. *J. Bionic Eng.* **2008**, *5*, 46–52. [CrossRef]
15. Kovalov, V.; Antonenko, Y.; Dašić, P. Method of structural design of heavy machine tools. *Proc. Technol.* **2016**, *22*, 146–152. [CrossRef]

16. Sharma, A.; Thapa, S.; Goel, B.; Kumar, R.; Singh, T. Structural analysis and optimization of machine structure for the measurement of cutting force for wood. *Alex. Eng. J.* **2023**, *64*, 833–846. [CrossRef]
17. Kiyono, C.Y.; Picelli, R.; Sivapuram, R.; De Leon, D.M.; Silva, E.C.N. Stress-based topology optimization approach using binary variables and geometry trimming. Finite Elem. *Anal. Des.* **2023**, *227*, 104044.
18. Amaral, R.R.; Borges, J.A.; Gomes, H.M. Proportional Topology Optimization under Reliability-based Constraints. *J. Appl. Comput. Mech.* **2022**, *8*, 319–330.

Disclaimer/Publisher's Note: The statements, opinions and data contained in all publications are solely those of the individual author(s) and contributor(s) and not of MDPI and/or the editor(s). MDPI and/or the editor(s) disclaim responsibility for any injury to people or property resulting from any ideas, methods, instructions or products referred to in the content.